Chemical Engineering Journal 165 (2010) 175–183

Contents lists available at ScienceDirect

Chemical Engineering Journal

journal homepage: www.elsevier.com/locate/cej

Formation of dynamic membrane in an anaerobic membrane bioreactor for municipal wastewater treatment

Xinying Zhang[a], Zhiwei Wang[a,*], Zhichao Wu[a], Fenghai Lu[a], Jun Tong[a], Lili Zang[b]

[a] Key Laboratory of Yangtze River Water Environment of Ministry of Education, College of Environmental Science and Engineering, No. 1239 of Siping Rd., Tongji University, Shanghai 200092, PR China
[b] Shanghai Zizheng Environmental Technology Co. Ltd., Shanghai 200437, PR China

ARTICLE INFO

Article history:
Received 4 July 2010
Received in revised form 7 September 2010
Accepted 13 September 2010

Keywords:
Anaerobic dynamic membrane bioreactor
Dacron mesh
Filtration
Wastewater treatment

ABSTRACT

An anaerobic dynamic membrane bioreactor with a high flux of 65 L/(m^2 h) was used to treat municipal wastewater. Particle size distribution, scanning electron microscopy, gel filtration chromatography (GFC), and three-dimensional excitation–emission matrix (EEM) were used to investigate the components of the cake layer formed on the membrane surface and the interception effect of the dynamic membrane. Test results showed that the dynamic membrane was formed by suspended solids (SS) in the settling zone and the soluble contents such as soluble microbial products (SMP) and extracellular polymeric substances (EPS). According to the index of SS/cake volume, the formation of dynamic membrane can be divided into three stages, i.e., the formation of separation layer, the stable growth stage, and the fouling stage. The accumulation rates of SS, SMP and EPS were of some differences at each stage. The secondary membrane was not entirely formed until the 7th day, and the dynamic membrane demonstrated a weak interception effect of dissolved organic matters after the 20th day. From EEM and GFC analyses of SMP in the cake layer, it was found that the fluorescence intensity ratio of Peak B/Peak A in the EEM fluorescence spectra had a similar changing tendency with large molecules of MW > 5000 kDa. They both increased with operation time before the 20th day, probably due to the soluble by-products secreted by the microorganism in the cake layer.

1. Introduction

In the past years, the aerobic activated sludge process has been the dominant technology for treating municipal wastewater. However, due to the high costs of aeration and sludge handling in aerobic treatment, anaerobic process demonstrates its advantages in municipal wastewater treatment [1,2]. Biomass retention is a very important factor for anaerobic treatment of municipal wastewater mainly due to the low growth rate of anaerobic microorganisms, particularly during low temperature period when the degradation rate (hydrolysis) of suspended solids (SS) and colloidal fractions is the rate limiting step [3–5].

With the development of membrane technology, the integration of membrane into bioreactor attracted more attention. Anaerobic membrane bioreactor (AnMBR) can achieve high-efficient solid–liquid separation and thus enable the independent control of hydraulic retention time (HRT) and sludge retention time (SRT). As a consequence, the particulate organics retained in the reactor can eventually be hydrolyzed and degraded because of the long solids retention time [6,7]. In practical applications of AnMBRs, there are still obstacles such as high cost of membrane module, low membrane flux, rapid membrane fouling, etc. [2]. Dynamic membrane technology may be a promising approach to resolve these problems. Dynamic membrane, which is also called secondary membrane, is formed on the underlying support material when the filter solution contains fine particles [8]. The membrane itself may be no longer necessary, since solids rejection will be accomplished by the cake layer which can be formed and re-formed in situ. Once the membrane is severely fouled, the dynamic layer can be removed and replaced by a new deposited layer. Thus, the expense of purchasing and physically replacing new membrane is spared [9]. To date, there have been many studies focusing on the use of meshes or fabrics as the support material for solid–liquid separation in the aerobic wastewater treatment. Chu and Li [10] used the industrial filter cloth material and found that the permeate turbidity was less than 9 NTU, SS was zero and cake layer was the major resistance factor. Fan and Huang [11] reported that the biomass layer of the dynamic membrane on mesh consisted of a cake layer and a gel layer. The gel layer had a structure like conventional membranes and played a key role in the permeability of the dynamic membrane. Liu et al. [12] divided the formation process of dynamic membrane into four stages based on the flux behaviors under constant filtra-

* Corresponding author. Tel.: +86 21 65980400; fax: +86 21 65980400.
E-mail address: zwwang@tongji.edu.cn (Z. Wang).

1385-8947/$ – see front matter © 2010 Elsevier B.V. All rights reserved.
doi:10.1016/j.cej.2010.09.013

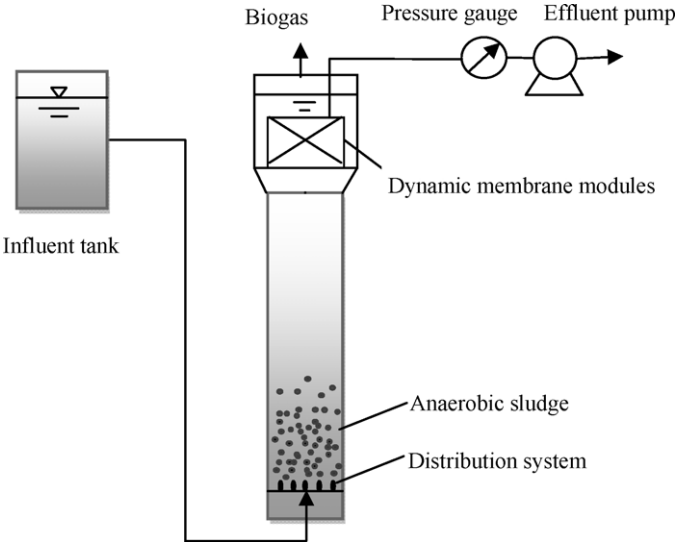

Fig. 1. Diagram of the AnDMBR.

tion pressure, i.e., substrate formation, separation layer formation, fouling layer formation and filtration cake formation.

These results may be not applicable to anaerobic dynamic membrane bioreactors (AnDMBR) treating low strength organic wastewater such as municipal wastewater due to the distinct differences from aerobic treatment processes. Some attempts on the AnDMBR have been made [13,14] in order to clarify its behaviors and characteristics in wastewater treatment. However, only low levels of flux were achieved (<5 L/(m^2 h)), which would be a bottleneck to the practical engineering application of AnDMBR. Generally speaking, the research on AnDMBR is still limited and worth further studying. The purpose of this study, therefore, is to investigate the formation process of dynamic membrane at a high flux of about 65 L/(m^2 h) in an AnDMBR for municipal wastewater treatment. The accumulation and variations of SS, soluble microbial products (SMP) and extracellular polymeric substances (EPS) on the membrane surface were investigated in order to gain a deep understanding on the formation mechanisms of the dynamic membrane in the AnDMBR.

2. Materials and methods

2.1. Operation of AnDMBR

The experimental setup used in this study is shown in Fig. 1. The AnDMBR system, which had an effective volume of 45 L and an average HRT of 8 h, consisted of a settling zone (upper part) and an upflow anaerobic sludge blanket (UASB) reactor (lower part). Flat-sheet dynamic membrane modules were mounted in the settling zone, which were made of Dacron mesh (pore size = 61 μm). The dynamic membrane modules were kept at a high flux of about 65 L/(m^2 h). The water level in the bioreactor was controlled by an elevated influent tank to maintain a constant water level. The membrane-filtered effluent was then obtained by using a peristaltic pump connected to the modules. The effluent flow rate and the trans-membrane pressure (TMP) were monitored by a water meter and a pressure gauge, respectively. The temperature in the reactor was in the range of 10–15 °C during the experiment (in the seasons of autumn and winter). The effluent pH of the AnDMBR was in the range of 7.2–7.6.

In the experiment, the effluent of aerated grit chamber of Shanghai Quyang municipal wastewater treatment plant was adopted as the influent of the AnDMBR, the characteristics of which are summarized in Table 1.

Table 1
The characteristics of the influent wastewater[a].

Water quality parameters	Concentration
COD (mg/L)	302.1 ± 87.9
NH_4^+-N (mg/L)	37.9 ± 8.6
TN (mg/L)	58.8 ± 10.2
SS (mg/L)	120 ± 23
pH	7.3 ± 0.3
Water temperature (°C)	10–15

[a] Values are given as mean concentration ± standard deviation; number of measurements: n = 30.

2.2. Analytical methods

2.2.1. Cake layer collection and filtration resistance

Several dynamic membrane modules were placed in the AnDMBR and periodically taken out at different fouling stages. Once a used module was taken out, a new module was placed in for maintaining a constant HRT of the bioreactor. The cake layer on the membrane surface was carefully scraped off by a plastic sheet and simultaneously rinsed with distilled water. The collected samples were placed on a magnetic blender (Model JB-2, Leici Instrument Incorporated, Shanghai, China) and well mixed. After that, the collected samples were diluted with distilled water and could be used for further analysis.

The filtration resistance at each step was calculated using the following equation:

$$R_t = R_m + R_c + R_p = \frac{\mathrm{TMP}}{\mu J} \times 3600 \quad (1)$$

where R_t is the total membrane resistance (m^{-1}), R_m is the intrinsic resistance of Dacron mesh (m^{-1}), R_c is the cake layer resistance (m^{-1}), R_p is the pore-clogging resistance (m^{-1}), J is the instantaneous flux (m^3 m^{-2} h^{-1}), TMP is the trans-membrane pressure (Pa), and μ is the dynamic viscosity of permeate water (Pa s). R_t was calculated at the each stage of the filtration experiment. The method described by Fan and Huang [11] was adopted for the measurement of the R_m and R_p. R_p was obtained by subtracting the R_m from the resistance of a dynamic membrane module after physical cleaning by tap water; R_c could be calculated by subtracting the filtration resistance of R_m and R_p from R_t.

2.2.2. Scanning electron microscopy (SEM)

The dynamic membrane module was taken out from the AnDMBR. A piece of membrane was then cut from the middle of the fouled membrane module. The sample was naturally air-dried and coated with aurum–platinum alloy (with coating depth 10 nm), and then observed using the SEM (Model XL-30, Philips, Netherlands).

2.2.3. Particle size distribution (PSD) analysis

PSD of the sample was carried out by a focused beam reflectance measurement (EyeTech particle size and shape analyzer, Ankersmid, Holland).

2.2.4. Extraction of SMP and EPS of cake layer

The collected cake layer was centrifuged at 6000 rpm for 30 min and then the extracted supernatant was filtrated through a membrane with a mean pore size of 0.45 μm. The filtrate of the centrifuged supernatant was regarded as SMP. The remaining pellet was washed and re-suspended with saline water (0.9% NaCl solution). The mixed liquor was then subject to heat treatment (100 °C, 1 h) and centrifuged again under the same operating conditions. The centrifuged supernatant was regarded as the EPS solution [15].

SMP and EPS concentrations were measured as polysaccharides and proteins. Polysaccharides were measured using the Anthrone method as described by Dubois et al. [16] with a glucose standard, and proteins were determined by a modified Lowry method [17] with BSA (bovine serum albumin, Sigma fraction V, 96%) as a standard.

2.2.5. Gel filtration chromatography (GFC) analysis

The molecular weight (MW) distributions of samples were determined by a GFC analyzer (SHIMADZU Co., Japan). A TSK G4000SW type gel column (TOSOH Corporation, Japan), which was heated to 40 °C and maintained by thermostat control (CTO-10ASvp), was used in this work with pure water as eluent at a flow rate of 0.5 mL min^{-1}. The samples were filtered with a 0.45 μm hydrophilic filtration membrane prior to the injection (50 μL) and analyzed using a refractive index detector (RID-10A). The MW was calculated according to the calibration with standard polyethylene glycols (PEGs) of MW 194 Da, 620 Da, 4020 Da, 11,840 Da, 62,100 Da, 128,000 Da, and 771,000 Da (Merck Corporation, Germany) using the GFC for Class VP software package included with Class VP 5.03 software (SHIMADZU Co., Japan). In this study, the GFC calibration curve for the MW versus the elution peak time (t) was as follows:

$$\text{Log(MW)} = -0.318t + 9.4553 \quad (2)$$

2.2.6. Three-dimensional excitation–emission matrix (EEM) fluorescence spectra analysis

Fluorescence measurements were conducted using a luminescence spectrometry (F-4500 FL spectrophotometer, Hitachi, Japan). The spectrometer used a xenon excitation source, and slits were set at 10 nm for both excitation and emission. To obtain fluorescence EEM spectra, excitation wavelengths were incremented from 200 to 600 nm at 5 nm steps; for each excitation wavelength, the emission spectrum was detected from 200 to 600 nm at 5 nm steps. Scan speed was set at 2400 nm/min. A 290 nm emission cutoff filter was used in scanning to eliminate the second order Raleigh light scattering. The spectra of sealed distilled water were recorded as the blank. The software Origin 7.5 (OriginLab Corporation, USA) was employed for handling the EEM data. The EEM spectra were plotted as the elliptical shape of contours. The *X*-axis represented the emission spectra from 200 nm to 550 nm while the *Y*-axis indicated the excitation wavelength from 200 nm to 400 nm, and the third dimension, i.e., the contour line, was shown to express the fluorescence intensity (FI) at an interval of 5.

2.2.7. Other item analysis

Measurements of chemical oxygen demand (COD), ammonium (NH_3-N), total nitrogen (TN), pH, SS and volatile suspended solids (VSS) were performed according to Chinese NEPA standard methods [18].

3. Results and discussion

3.1. Pollutants removal performance in the AnDMBR

The AnDMBR was operated for nearly 100 days, and a stable COD removal efficiency of 57.3 ± 6.1% was achieved (see Fig. 2). The effluent COD concentration was 120.8 ± 34.0 mg/L when the influent COD concentration fluctuated from 159.0 mg/L to 500.0 mg/L. During the experiment period, the effluent SS concentration was in the range of 0–15 mg/L (number of measurements: n = 10). Average biomass concentration in the UASB reactor varied from 5.9 g VSS/L to 19.8 g VSS/L, while the SS in settling zone increased from 68 mg/L to 250 mg/L from the beginning to the end of the experiment.

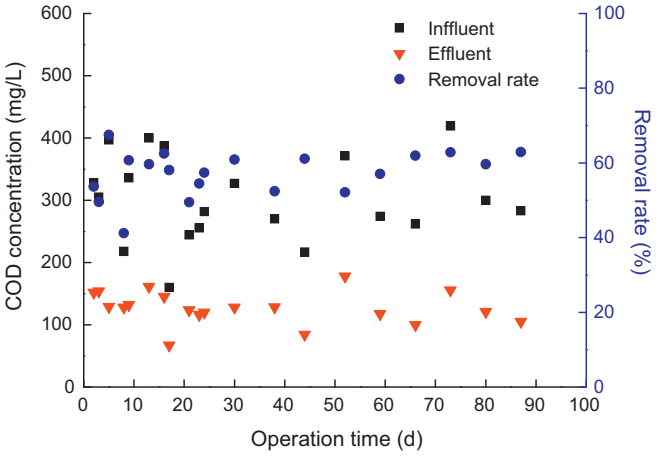

Fig. 2. COD concentration variations of the system during the experiment.

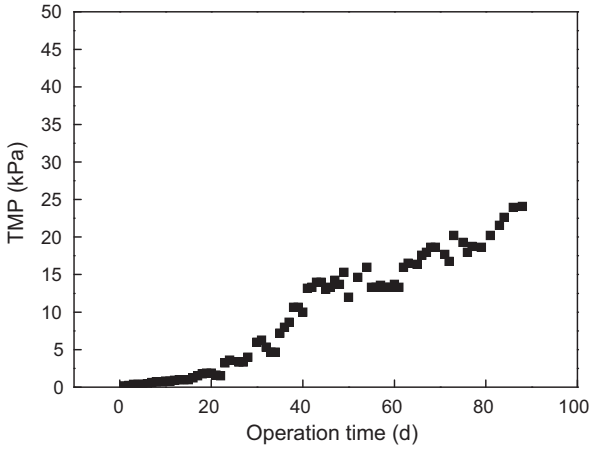

Fig. 3. Variations of TMP during the experiment.

The COD removal efficiency was (56.6 ± 8.26)% (n = 8) before day 20 and increased to (57.7 ± 4.6)% (n = 12) after the formation of cake layer on day 20. The improvement of COD removal after the formation of dynamic membrane was very limited in this AnMBR, indicating that the dynamic membrane of AnMBR cannot effectively retain the soluble COD. The major role of dynamic membrane in AnMBR was to remove particles (or particulate COD). Therefore, the downstream treatment is needed to remove the soluble COD contained in the AnMBR effluent.

3.2. Formation and filtration capacity of the dynamic membrane

The variations of TMP with operation time are demonstrated in Fig. 3. It can be observed that the TMP increased slowly with operation time as membrane flux was kept at about 65 L/(m^2 h) during the experiment. When the flux decreased, physical cleaning by tap water was carried out to remove fouling layer and to recover the membrane permeability. Afterwards, another operation period was started.

The filtration resistances of cake layer of the dynamic membrane in the whole filtration period were calculated with above-mentioned methods and the results are shown in Table 2. The R_m

Table 2
A series of resistances of the dynamic membrane with flux 65 L/(m^2 h).

Operation time (day)	2	5	7	20	48	88
R_c ($\times 10^{10}$ m^{-1})	1.1	1.8	3.1	9.4	69.0	121.2

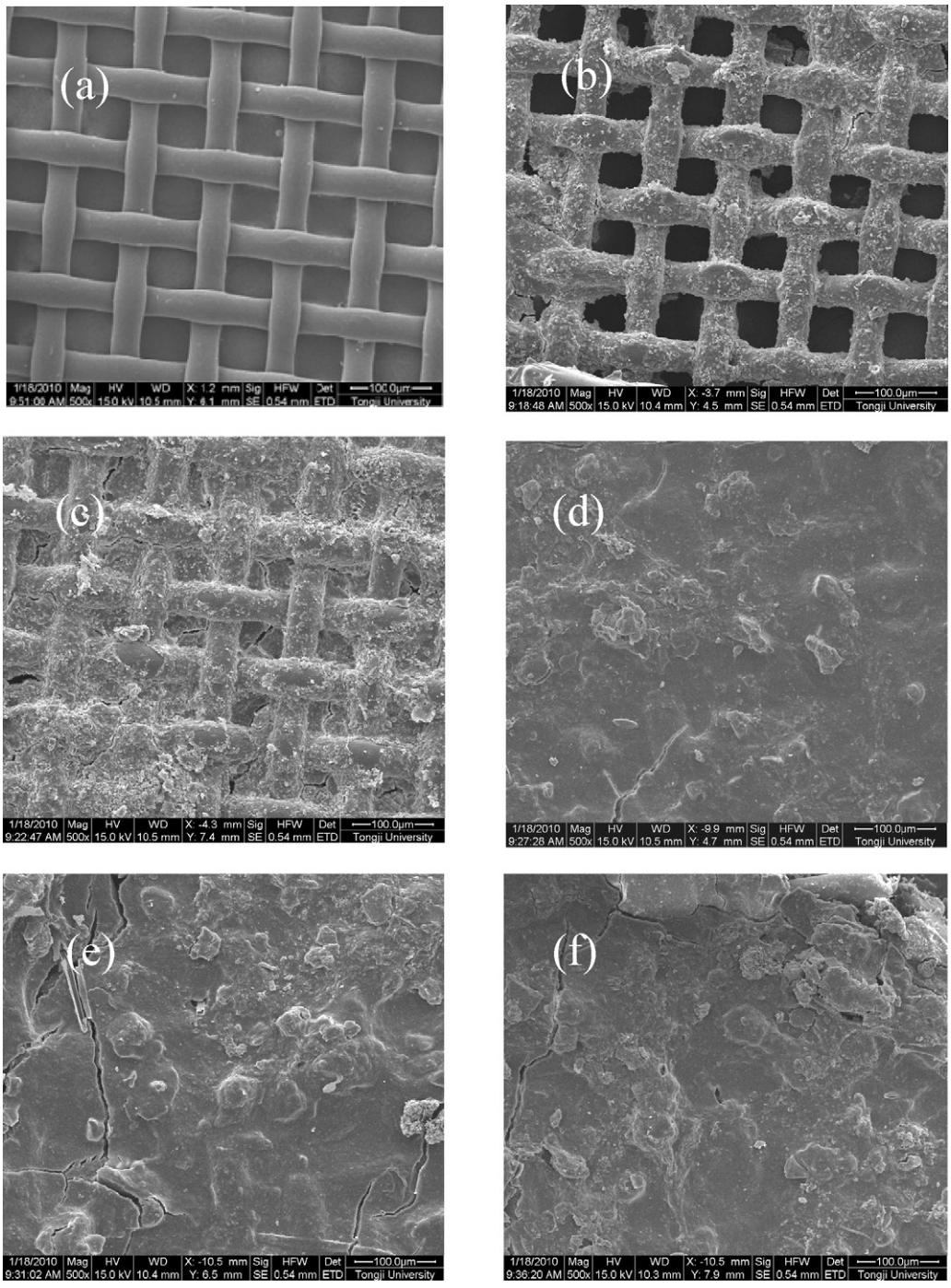

Fig. 4. SEM photographs of: (a) clean membrane surface; (b) fouled membrane surface (2 days); (c) fouled membrane surface (7 days); (d) fouled membrane surface (20 days); (e) fouled membrane surface (48 days); (f) fouled membrane surface (88 days).

was $3.8 \times 10^7\ m^{-1}$. The R_p value was about $1.3 \times 10^7\ m^{-1}$, which did not change with the increase of operation time.

It is shown in Table 2 that the intrinsic resistances of the Dacron mesh and the resistances of pore-clogging were much smaller compared to the filtration resistance of cake layer. The cake layer played a major role in the increase of filtration resistance with the increase of operation time, which is consistent with the research of Hwang and Cheng [19].

The SEM photographs of dynamic membrane surfaces at different fouling stages are shown in Fig. 4. As can be seen from Fig. 4(a), the surface of unused Dacron mesh was smooth. With the interception of some sludge particles in the initial filtration process, the secondary membrane was not entirely formed until the 7th day. The cake layer at that time was porous and uneven. Then the cake layer became thicker and more compacted, which can be seen from Fig. 4(d–f). In this process, the increase of resistance was due to both the thickness-increase resistance and the compaction resistance [20].

The dynamic membrane was mainly formed by SS deposited on the membrane surface in the filtration process. The variations of SS on the dynamic membrane surface are shown in Fig. 5(a). It can be found that SS deposited on the membrane surface increased continuously with the operation time, which could be attributed to the lack of cross-flow in the settling zone. The accumulation of SS was

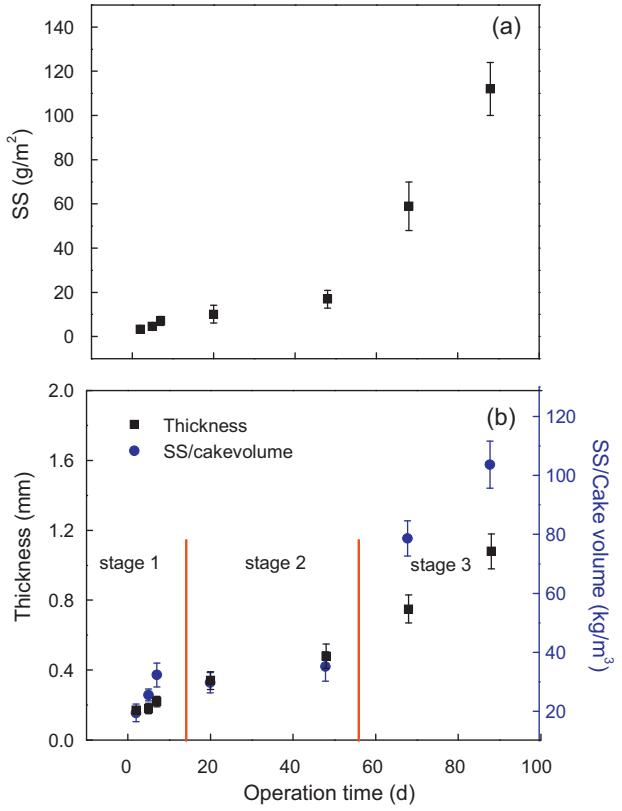

Fig. 5. Change of the cake layer on the dynamic membrane surface with the operation time. (a) SS mass per unit area of membrane surface; (b) thickness of the cake layer and SS/cake volume ($n = 5$).

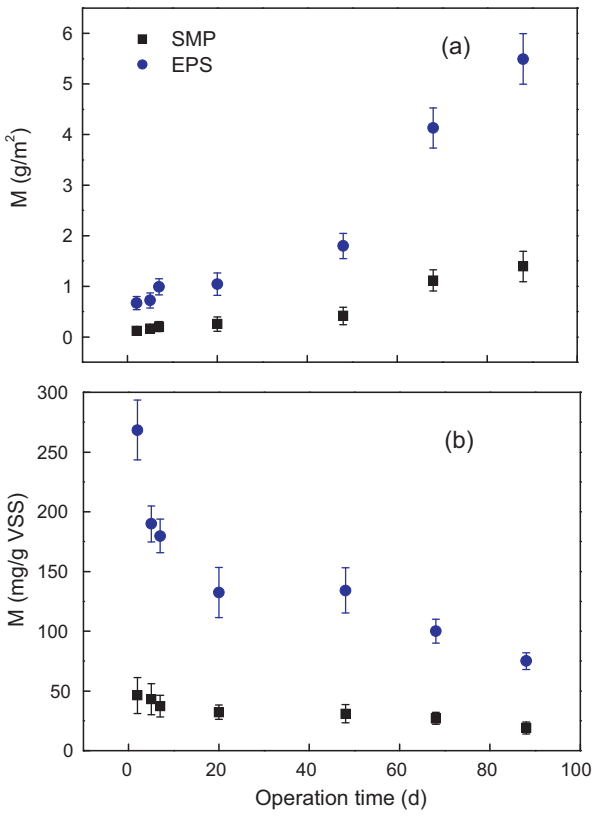

Fig. 6. Change of the cake layer on the dynamic membrane surface with the operation time. (a) SMP and EPS on the membrane surface; (b) SMP and EPS content of the cake layer ($n = 5$).

a major factor responsible for the increase of filtration resistance. Besides that, another important factor influencing membrane resistance was the layer compaction [19]. The index of SS/cake volume can reflect the compaction and porosity of the cake layer. The variations of thickness and SS/cake volume against operation time are illustrated in Fig. 5(b). From Fig. 5(b), it can be found that, as a secondary membrane, the formation of the cake layer might be roughly divided into three stages as follows. (1) The formation of separation layer: SS with the size similar to the mesh in the settling zone were intercepted by the mesh, filling into mesh holes. Then the hydrophobic mesh was changed to be hydrophilic by the deposition of hydrophilic sludge [11] and the quick accumulation of SS led to an initial separation layer. (2) The stable growth stage: the mass and thickness of the cake layer increased synchronously and its SS/cake volume had little change. (3) The fouling stage: with the increasing of filtration pressure, the growth of SS surpassed that of thickness and its SS/cake volume thus increased, indicating the compaction of cake layer and the dramatic increase of filtration resistance.

The dynamic membrane was not only formed by sludge particles, but also by the interception of the soluble and colloidal contents such as SMP and EPS in dynamic membrane during filtration [13]. The content of these substances on the dynamic membrane surface is shown in Fig. 6.

From Fig. 6(a), it can be found that the mass of SMP and EPS on the membrane surface both increased with the operation time, similar to the accumulation of SS. Previous studies [21–25] showed that the accumulation of SMP and EPS demonstrated significant influences on the characteristics of cake layer on the membrane surface. Sludge adhesion could be enhanced by polymeric interactions. Moreover, it can be observed that the content of SMP and EPS per unit mass of VSS in the initial cake layer was higher than that of later stage (see Fig. 6(b)). It is mainly due to the fact that SMP and EPS have macromolecules which are more readily attached to the membrane surfaces by permeation drag [26]. The results were of some similarities with aerobic membrane bioreactors. The sludge particles with higher SMP and EPS content preferentially adhered to the surface, and then other particles could be retained by the dynamic membrane by the permeation drag. However, some differences still existed. In the aerobic membrane bioreactor, due to the cross-flow on the membrane surface, sludge particles with larger size could not deposit on membrane surfaces and soluble macromolecules played an important role in the initial separation layer as a gel layer [11]. However, in the AnDMBR, the separation layer mainly consisted of sludge particles intercepted by the membrane due to the weak disturbance on the membrane surface.

3.3. PSD analysis

The volume average diameters of particles in the influent, the mixed liquid in settling zone are shown in Table 3. At the initial operational stage, the particles size in the effluent had an obvious trend of decrease, and more fine particles were intercepted. In the effluent of the 7th day and 20th day, the volume average diameter of particles was just $11.3 \pm 5.3\,\mu m$ and $9.8 \pm 3.6\,\mu m$. Along with the filtrating, the cake layer became dense and less porous. For the single-layer structure of the Dacron mesh, some foulants on the surface might pass though the pores under high suction pressures of the peristaltic pump. It resulted in that particles with larger size appeared in the effluent of the 48th day (with volume average diameter of $18.9 \pm 7.3\,\mu m$) and even larger in the effluent of the 88th day (with volume average diameter of $22.9 \pm 8.1\,\mu m$) at the end of fouling stage.

Table 3
Volume average diameter of samples[a].

Sample	Influent	Settling zone[b]	Effluent (2 days)	Effluent (5 days)	Effluent (7 days)	Effluent (20 days)	Effluent (48 days)	Effluent (88 days)
Volume average diameter (μm)	115.6 ± 17.3	96.8 ± 10.9	77.8 ± 9.6	43.7 ± 12.6	11.3 ± 5.3	9.8 ± 3.6	18.9 ± 7.3	22.9 ± 8.1

[a] Values are given as mean concentration ± standard deviation; $n = 5$.
[b] The dynamic membrane modules were set in the settling zone.

3.4. GFC analysis

GFC is a useful technique for evaluating various water treatment processes [27]. Dissolved organic matters (DOM) are eluted through a porous solid phase; large molecules are unable to penetrate the pores and thus elute more quickly than small molecules [28].

The GFC chromatograms of the DOM in the supernatant of the settling zone and the effluent are shown in Fig. 7. It can be seen that the GFC chromatograms of the two samples were similar but with some differences of the peak locations along with the filtration process. Before the 7th day, the chromatograms showed little differences, indicating that the dynamic membrane had no removal effect of soluble organic matters in the initial stage. It also can explain that the high SMP and EPS contents in the initial cake layer could be attributed to the attachment on the support materials rather than the interception effect.

Along with the formation of cake layer, the dynamic membrane showed an interception effect with a right shift of the peak locations (on the 20th and 48th day) or reduced intensity of peak 1 (on the 88th day) in the effluent. This interception effect of DOM could be attributed to the accumulation of SS mass and the increasing compaction of cake layer with the operation time, which has been reported to be the important factors determining the rejection of large molecules [19].

Moreover, the MW distribution of SMP in the cake layer at different filtration stages was also investigated to obtain a deep insight of the characteristics of the cake layer (see Fig. 8). There were three peaks in these samples. It was found that these peak locations had a tendency of moving to shorter elution time with operation time, indicating the accumulation of large molecules in the cake layer.

In order to better understand GFC chromatograms of SMP in the cake layers of the AnDMBR, the MW distributions of these samples

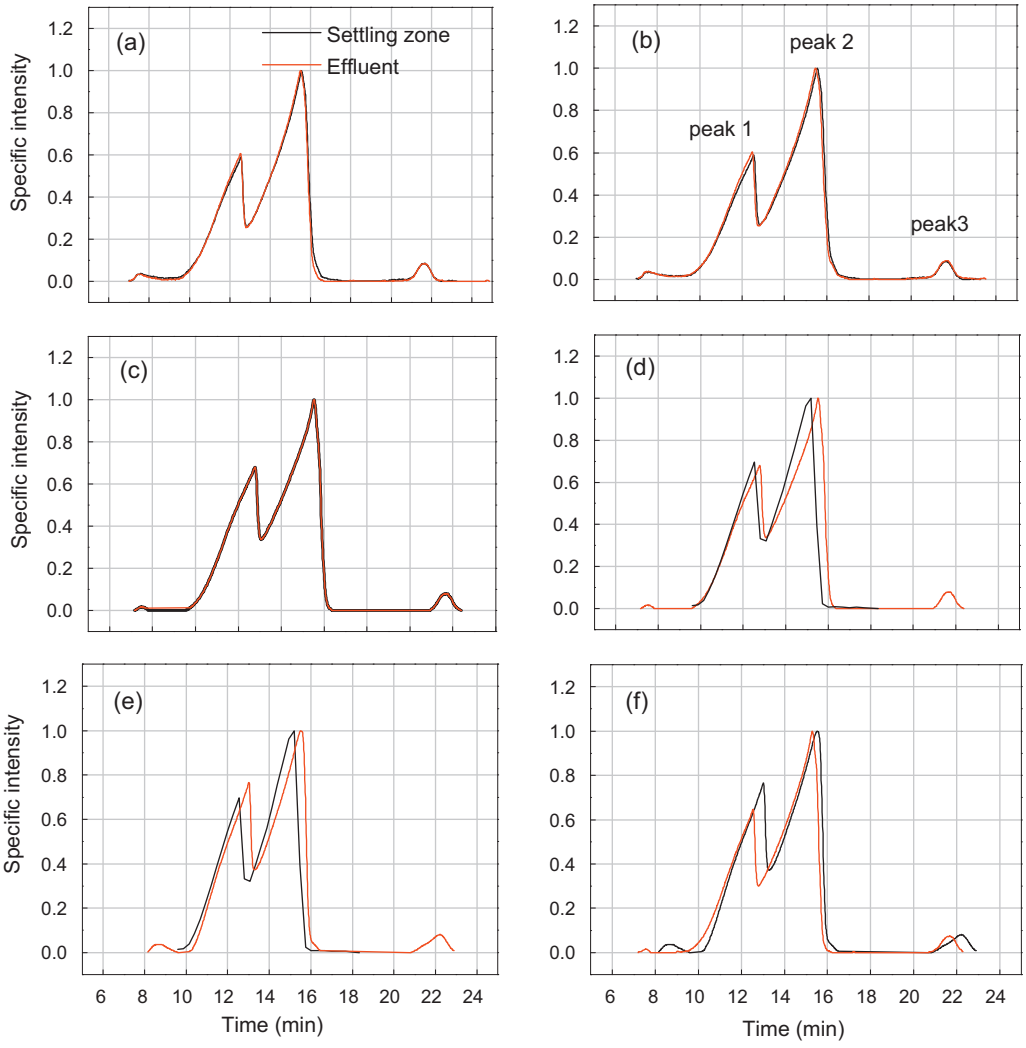

Fig. 7. GFC chromatograms of DOM in the settling zone and effluent on (a) the 2nd day; (b) the 5th day; (c) the 7th day; (d) the 20th day; (e) the 48th day; (f) the 88th day.

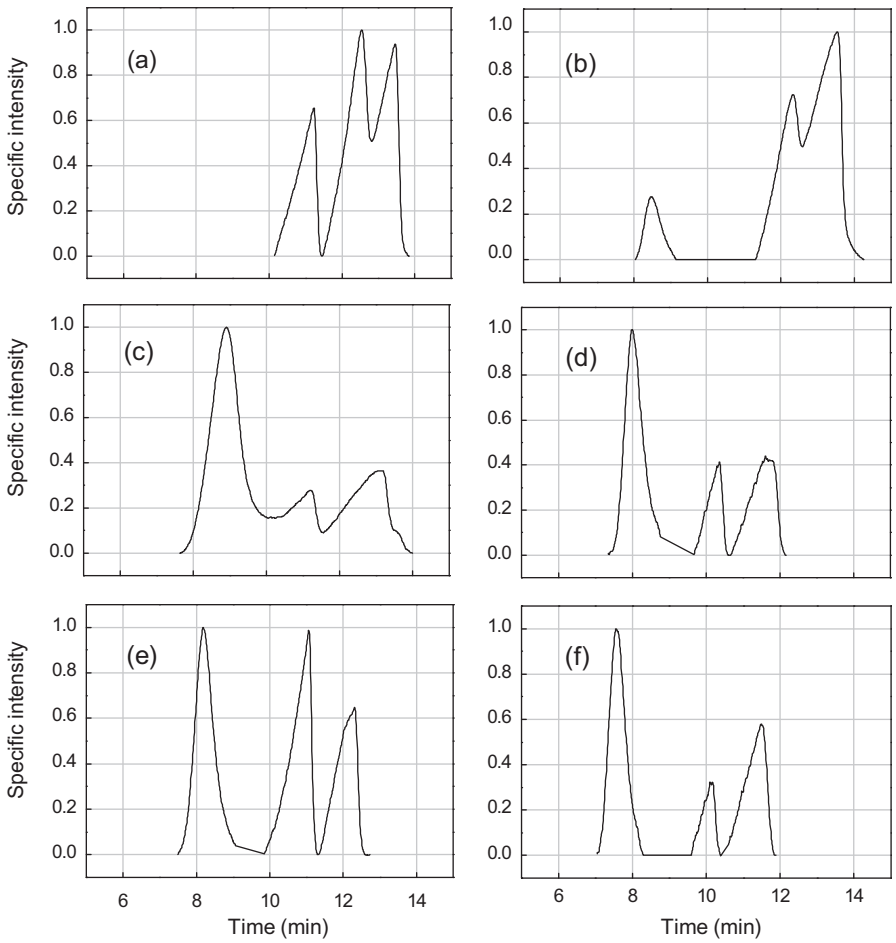

Fig. 8. GFC chromatograms of SMP of cake layer on (a) the 2nd day; (b) the 5th day; (c) the 7th day; (d) the 20th day; (e) the 48th day; (f) the 88th day.

are illustrated in Fig. 9. It can be seen that on the 2nd day, the SMP in the cake layer mainly consisted of molecules of MW < 5000 kDa. Afterwards, molecules of MW > 5000 kDa appeared and accumulated in the cake layer, increasing from 6.9% on the 5th day to 51.5% on the 20th day. For the lack of removal effect of DOM by the initial cake layer as mentioned above in the GFC analysis of the DOM in the supernatant and the effluent, this accumulation effect of large molecules in SMP cannot be attributed to interception effect. It was reported that the increasing of cake layer thickness might result in endogenous decay or cell lysis occurring at the bottom layer for the poor transfer of nutrients from the bulk solution [29]. Then the soluble macromolecules were released and accumulated in the cake layer. However, after the 20th day, SMP in the cake layer of molecules of MW < 500 kDa increased constantly, which might be due to the interception effect of DOM by the dynamic membrane after the 20th day.

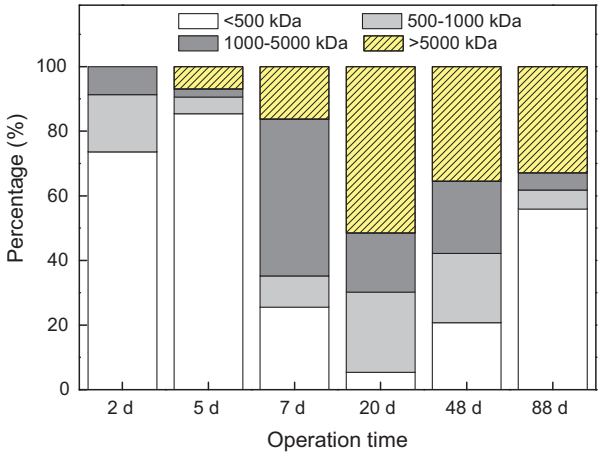

Fig. 9. GFC distribution of SMP in the cake layer.

3.5. EEM analysis

The EEM spectra give spectral information about the chemical compositions such as humic-like, tyrosine-like, tryptophan-like or phenol-like organic compounds, which have fluorescence characteristics in the samples [30].

Fig. 10 shows EEM fluorescence spectra of SMP in the cake layer. Two peaks were readily identified from the EEM fluorescence spectra. The first main peak was identified at the excitation/emission wavelengths (Ex/Em) of 230–240 nm/335–350 nm (Peak A), which was related to aromatic protein-like substances [31]. The second main peak located at the Ex/Em of 280 nm/315–335 nm (Peak B) was described as tryptophan protein-like substances [32], and was associated with the soluble microbial by-products [31]. Fluorescence parameters, such as peak location, FI and different peak intensity ratios, were obtained from the EEM fluorescence spectra are listed in Table 4. The intensity ratio of Peak B/Peak A (B/A) reflected the constituents of the protein-like substances [32].

The total FI was calculated as FI per unit of membrane area (FI_T). From Table 4, we can see that FI_T of Peak A (FI_A) and Peak B (FI_B) showed different variations with the operation time. The increasing rate of FI_B exceeded that of FI_A, while their sum $FI_{(A+B)}$ grew

Table 4
Fluorescence parameters of SMP in the cake layer.

Operation time	Peak A		Peak B		FI_T			B/A
	Ex/Em	FI	Ex/Em	FI	FI_A	FI_B	$FI_{(A+B)}$	
2	230.0/340.0	92.2	280.0/325.0	90.9	174.7	172.3	346.9	0.99
5	230.0/340.0	101.7	280.0/335.0	160.4	192.6	303.8	496.4	1.58
7	230.0/340.0	81.7	280.0/330.0	142.6	206.3	360.1	566.4	1.75
20	235.0/335.0	71.5	280.0/335.0	183.6	180.5	463.6	644.1	2.57
48	230.0/335.0	56.0	285.0/335.0	132.9	211.8	503.4	715.3	2.38
68	230.0/335.0	61.0	280.0/335.0	141.0	308.1	712.1	1020.2	2.31
88	230.0/330.0	67.8	280.0/335.0	159.8	428.1	1008.8	1436.9	2.36

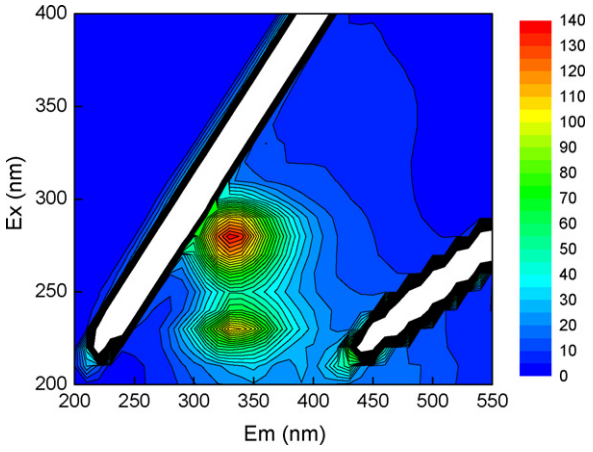

Fig. 10. EEM fluorescence spectra of SMP in the cake layer.

continuously. It was also found that the index of B/A increased before the 20th day and then decreased slightly, showing a similar tendency with molecules of MW > 5000 kDa in SMP of the cake layer. Therefore, it can be inferred that the accumulation of these large molecules (MW > 5000 kDa) was probably due to the soluble by-products secreted by the microorganism (represented by Peak B) in the cake layer. When the interception effect of DOM occurred after the 20th day, the accumulation of both two kinds of protein-like substances on the dynamic membrane surface resulted in a slight decrease of B/A. It can be concluded that the variations of SMP fluorescence in the cake layer on the dynamic membrane were attributed to the two factors, i.e., microorganism secretion and interception effect.

4. Conclusions

Dynamic membrane was applied in an anaerobic membrane bioreactor at a high flux of 65 L/(m^2 h) and its formation mechanisms were studied. The results showed that the dynamic membrane was formed by the sludge particles and the solutes and colloids content such as SMP and EPS. According to the index of SS/cake volume, the accumulation process could be divided into three stages of the formation of separation layer, the stable growth stage, and the fouling stage.

At the first stage, SS, SMP, EPS had a rapid accumulation on the membrane surface. The particles had a decrease trend in the effluent by the interception of dynamic membrane and no removal effect of DOM was found. At the second stage, the cake layer on the membrane surface showed a stable growing rate, with little change of SS/cake volume. The dynamic membrane showed a weak interception effect of DOM. At the third stage, the growth of SS surpassed that of thickness, indicating the compaction of cake layer. Particles with large size were present in the effluent under the high suction pressure.

From EEM and GFC analysis of SMP in the cake layer, it was found that the index of B/A increased before the 20th day. It showed a similar tendency with large molecules of MW > 5000 kDa, which were mainly originated from the soluble by-products secreted by the microorganism in the cake layer. When the interception effect of DOM occurred after the 20th day, it was found that B/A and molecules of MW > 5000 kDa both had a slight decrease.

Acknowledgements

Financial support of this work by the Key Special Program on the S&T for the Pollution Control and Treatment of Water Bodies (2008ZX07316-002) and by the Science & Technology Commission of Shanghai Municipality fund (09dz1204200 and 08231200200) is gratefully acknowledged.

References

[1] Metcalf and Eddy Inc., Wastewater Engineering: Treatment and Reuse, 4th ed., McGraw-Hill, New York, 2003.
[2] B.Q. Liao, Anaerobic membrane bioreactors: applications and research directions, Crit. Rev. Environ. Sci. Technol. 36 (2006) 489–530.
[3] B. Lew, S. Tarre, M. Beliavski, C. Dosoretz, M. Green, Anaerobic membrane bioreactor (AnMBR) for domestic wastewater treatment, Desalination 243 (2009) 251–257.
[4] T.A. Elmitwalli, G. Zeeman, G. Lettinga, Anaerobic treatment of domestic sewage at low temperature, Water Sci. Technol. 44 (2001) 33–37.
[5] B. Lew, M. Belavski, S. Admon, S. Tarre, M. Green, Temperature effect on UASB reactor operation for domestic wastewater treatment in temperate climate regions, Water Sci. Technol. 48 (2003) 25–30.
[6] J. Grundestarn, D. Hellstrom, Wastewater treatment with anaerobic membrane bioreactor and reverse osmosis, Water Sci. Technol. 56 (2007) 211–217.
[7] P.R. Berube, E.R. Hall, P.M. Sutton, Parameters governing permeate flux in an anaerobic membrane bioreactor treating low-strength municipal wastewaters: a literature review, Water Environ. Res. 78 (2006) 887–896.
[8] V.T. Kuberkar, R.H. Davis, Modeling of fouling reduction by secondary membrane, J. Membr. Sci. 168 (2000) 243–258.
[9] D.W. Cao, H.Q. Chu, W. Jin, B.Z. Dong, Characteristics of the biodiatomite dynamic membrane (cake layer) for municipal wastewater treatment, Desalination 250 (2010) 544–547.
[10] L.B. Chu, S.P. Li, Filtration capability and operational characteristics of dynamic membrane bioreactor for municipal wastewater treatment, Sep. Purif. Technol. 51 (2006) 173–179.
[11] B. Fan, X. Huang, Characteristics of a self-forming dynamic membrane coupled with a bioreactor for municipal wastewater treatment, Environ. Sci. Technol. 36 (2002) 5245–5251.
[12] H.B. Liu, C.Z. Yang, W.H. Pu, J.D. Zhang, Formation mechanism and structure of dynamic membrane in the dynamic membrane bioreactor, Chem. Eng. J. 148 (2009) 290–295.
[13] D. Jeison, I. Díaz, J.B. van Lier, Anaerobic membrane bioreactors: are membranes really necessary? Electron. J. Biotechnol. 11 (2008) 1–7.
[14] Y. An, Z.W. Wang, Z.C. Wu, D.H. Yang, Q. Zhou, Characterization of membrane foulants in an anaerobic non-woven fabric membrane bioreactor for municipal wastewater treatment, Chem. Eng. J. 155 (2009) 709–715.
[15] I.S. Chang, C.H. Lee, Membrane filtration characteristics in membrane-coupled activated sludge system-the effect of physiological states of activated sludge on membrane fouling, Desalination 120 (1998) 221–233.
[16] M. Dubois, K.A. Grilles, J.K. Hamilton, P.A. Rebers, F. Smith, Colorimetric methods for determination of sugars and related substances, Anal. Chem. 28 (1956) 350–356.
[17] B. Frøund, R. Palmgren, K. Keiding, P.H. Nielsen, Extraction of extracellular polymers from activated sludge using a cation exchange resin, Water Res. 30 (1996) 1749–1758.
[18] Chinese NEPA, Water and Wastewater Monitoring Methods, 4th ed., Chinese Environmental Science Publishing House, Beijing, China, 2002.

[19] K.J. Hwang, Y.H. Cheng, The role of dynamic membrane in cross-flow microfiltration of macromolecules, Sep. Sci. Technol. 38 (2003) 779–795.
[20] H.Q. Chu, D.W. Cao, W. Jin, B.Z. Dong, Characteristics of bio-diatomite dynamic membrane process for municipal wastewater treatment, J. Membr. Sci. 325 (2008) 271–276.
[21] S. Tsuneda, H. Aikawa, H. Hayashi, A. Yuasa, A. Hirata, Extracellular polymeric substances responsible for bacterial adhesion onto solid surface, FEMS Microbiol. Lett. 223 (2003) 287–292.
[22] X. Huang, R. Liu, Y. Qian, Behaviour of soluble microbial products in a membrane bioreactor, Process Biochem. 36 (2000) 401–406.
[23] W. Lee, S. Kang, H. Shin, Sludge characteristics and their contribution to microfiltration in submerged membrane bioreactors, J. Membr. Sci. 216 (2003) 217–227.
[24] F.G. Meng, H.M. Zhang, F.L. Yang, S.T. Zhang, Y.S. Li, X.W. Zhang, Identification of activated sludge properties affecting membrane fouling in submerged membrane bioreactors, Sep. Purif. Technol. 51 (2006) 95–103.
[25] S. Liang, C. Liu, L.F. Song, Soluble microbial products in membrane bioreactor operation: behaviors, characteristics, and fouling potential, Water Res. 41 (2007) 95–101.
[26] T.H. Bae, T.M. Tak, Interpretation of fouling characteristics of ultrafiltration membranes during the filtration of membrane bioreactor mixed liquor, J. Membr. Sci. 264 (2005) 151–160.
[27] D.H. Seo, Y.J. Kim, S.Y. Ham, D.H. Lee, Characterization of dissolved organic matter in leachate discharged from final disposal sites which contained municipal solid waste incineration residues, J. Hazard. Mater. 148 (2007) 679–692.
[28] C.W.K. Chow, R. Fabris, J. van Leeuwen, D.S. Wang, M. Drikas, Assessing natural organic matter treatability using high performance size exclusion chromatography, Environ. Sci. Technol. 42 (2008) 6683–6689.
[29] B.K. Hwang, W.N. Lee, K.M. Yeon, P.K. Park, C.H. Lee, I.S. Chang, A. Drews, M. Kraume, Correlating TMP increases with microbial characteristics in the bio-Cake on the membrane surface in a membrane bioreactor, Environ. Sci. Technol. 42 (2008) 3963–3968.
[30] P.G. Coble, S.A. Green, N.V. Blough, Characterization of dissolved organic matter in Black Sea by fluorescence spectroscopy, Nature 48 (1990) 432–435.
[31] W. Chen, P. Westerhoff, J.A. Leenheer, K. Booksh, Fluorescence excitation–emission matrix regional integration to quantify spectra for dissolved organic matter, Environ. Sci. Technol. 37 (2003) 5701–5710.
[32] G.P. Sheng, H.Q. Yu, Characterization of extracellular polymeric substances of aerobic and anaerobic sludge using three-dimensional excitation and emission matrix fluorescence spectroscopy, Water Res. 40 (2006) 1233–1239.